Korean Jour. of Petrol. Geol. V. 11, No. 1, p. 9~17 2005

The Consideration for Optimum 3D Seismic Processing Procedures in Block II, Northern Part of South Yellow Sea Basin

대륙붕 2광구 서해분지 북부지역의 3D 전산처리 최적화 방안시 고려점

Seung-Won Ko (고승원)* · Kook-Sun Shin (신국선)* · Hyun-Young Jung (정현영)*

Abstract : In the main target area of the block II, large-scale faults occur below the unconformity developed around 1 km in depth. The contrast of seismic velocity around the unconformity is generally so large that the strong multiples and the radical velocity variation would deteriorate the quality of migrated section due to serious distortion. More than 15 kinds of data processing techniques have been applied to improve the image resolution for the structures formed from this active crustal activity. The bad and noisy traces were edited on the common shot gathers in the first step to get rid of acquisition problems which could take place from unfavorable conditions such as climatic change during data acquisition. Correction of amplitude attenuation caused from spherical divergence and inelastic attenuation has been also applied. Mild F/K filter was used to attenuate coherent noise such as guided waves and side scatters. Predictive deconvolution has been applied before stacking to remove peg-leg multiples and water reverberations. The velocity analysis process was conducted at every 2 km interval to analyze migration velocity, and it was iterated to get the high fidelity image. The strum noise caused from streamer was completely removed by applying predictive deconvolution in time space and τ-p domain. Residual multiples caused from thin layer or water bottom were eliminated through parabolic radon transform demultiple process. The migration using curved ray Kirchhoff-style algorithm has been applied to stack data. The velocity obtained after several iteration approach for MVA (migration velocity analysis) was used instead of DMO for the migration velocity. Using various testing methods, optimum seismic processing parameter can be obtained for structural and stratigraphic interpretation in the Block II, Yellow Sea Basin.

Keywords : 3D seismic processing, Block II, Yellow Sea Basin

요 약 : 2광구의 주요 탐사지역에는 심도 1 km 내외의 부정합면 하부에 대규모 단층이 발달되어 있다. 통상 이 부정합 인근의 탄성파 속도차는 매우 큰 편으로서 강한 다중반사파가 흔하게 발달되었고 탄성파 단면도는 왜곡되어 중합단면의 질적 저하가 예상되었다. 구조 인근의 다중반사파를 제거하고 해상력을 제고하기 위해 15가지 이상의 다양한 전산처리 기법이 적용되었다. 진폭 감소보정, 미약한 F/K 적용으로 일관성 잡음을 감쇠시켰다. 중합전 예측디콘볼루션으로 페그레그 다중반사파를 제거하였고 중합속도를 구하기 위해 매 2 km 간격으로 분석되었다. 잔여 다중반사파도 parabolic 라돈 변형절차를 거쳐 제거되었다. 중합자료를 얻기 위해 곡선파 curved ray Kirchhoff 형 알고리즘이 적용되었으며, MVA (migration velocity analysis)가 이용되었다. 결과적으로 자료 취득기간의 기상변화 등 취득시의 문제점으로 지적된 불량한 잡음이 섞인 트레이스는 최초로 CDP gathers에서 제거되었다. 이후 다수의 전산처리 기법을 써서 최적의 전산처리 변수가 구해졌으며 그 결과 서해대륙붕 2광구의 구조 및 층서 해석에 적합한 탄성파 단면도 획득을 위한 인자들을 얻을 수 있었다.

주요어 : 3차원 탄성파탐사자료처리, 2광구, 황해분지

Introduction

A time section and a two-dimensional depth-migration section were acquired for the block II area in 1997 and early 2004, respectively. The prospect in the block II area shows an unconformity at 1 km in depth with several big faults developed in its lower part. The layers in the sections are relatively steep, resulting in a structure with large contrast of horizontal velocity. The upper and lower parts of the unconformity generally have also a radical velocity variation. When a wave propagates through the region with large velocity contrast, the shape of the wavelet is highly distorted, causing the difficulty in building the velocity cube and imaging the substructure (Yilmaz, 1887). To resolve the difficulties, it is necessary to be of setting up the proper data processing sequence and selecting the optimum parameters.

The raw data used in this test processing was acquired in 2004 by Fugro-GeoTeam. Acquisition parameters in the data are as shown on Table 1.

The seismic data for block II area include a lot of linear noises, high frequency spike, water reverberation and peg-leg multiples caused from the thin layers, water bottom traps and side scatters - one of the coherent noises. Strum noise due to the streamer filled with oil is observed after 2000 ms of recording time.

In order to determine optimum processing parameters for the target area, more than 15 kinds of test processes have been performed for 2-D test lines.

*한국석유공사 (Korea National Oil Corp.), E-mail: shinks@knoc.co.kr

Table 1. Seismic acquisition parameters for 2004 3D, block 2 of the West Sea, 2004

Company	Fugro
Date Recorded	July, 2004
Shot interval	25 m, flip flop
Acquisition bin length	6.25 m
Acquisition bin width	25 m
No. of groups	288 × 5
Group interval	12.5 m
Near offset	185 m
Streamer separation	100 m
Record length	6 sec
Sampling rate	2 ms

The Test Processing Sequence

In order to determine optimum processing parameters for the block II area, test lines and processing sequences were set up as follows;

Step 1. Reformat
Step 2. Designature
Step 3. Trace edit
Step 4. Filtering
Step 5. Seismic and navigation merge
Step 6. True amplitude recovery
- Inelastic attenuation correction
- Spherical divergence correction

Step 7. Spike, swell and strum noise attenuation
- F/K filtering

Step 8. Multiple suppression
- Normal gaped deconvolution
- Predictive Deconvolution in τ-p domain

Step 9. Velocity analysis for adjacent trace summation
Step 10. Residual multiple suppression
- Parabolic radon demultiple

Step 11. Tidal static correction (if necessary)
Step 12. Velocity analysis for migration
Step 13. Migration
- Curved ray Kirchhoff prestack time migrartion

Step 14. Velocity analysis for stacking
Step 15. AGC
- Exponential gain amplitude correction

Step 16. NMO
Step 17. Stack
Step 18. Post stack Deconvolution
Step 19. Time variant filtering and scaling
Step 20. Residual static correction (if necessary)

The lines other than line 1475 have been used as 2-D test lines and Step 1~20 have been completed. In the first place, designature test was conducted to extract the source wavelet from seismic traces and to convert it to the minimum phase equivalent. Noisy and bad traces were removed by trace editing and 4 Hz low cut filter was applied. Fig. 1 shows the raw stack line, while Fig. 2 is the stack line after designature and low cut filtering process.

Spherical Divergence Correction and Inelastic Attenuation

The true amplitude recovery process was applied to

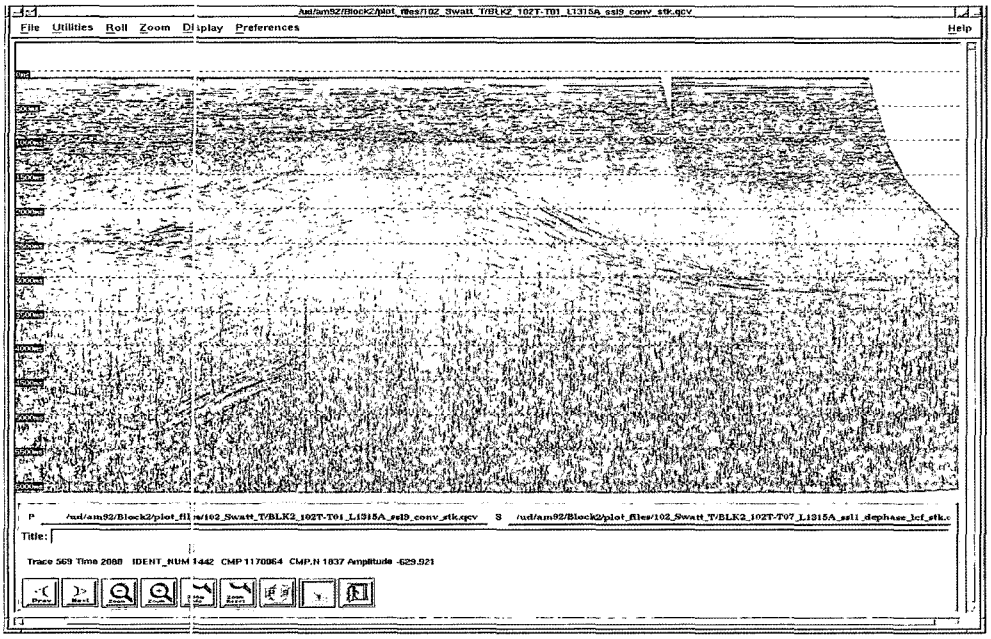

Fig. 1. Raw stack section for line 1315.

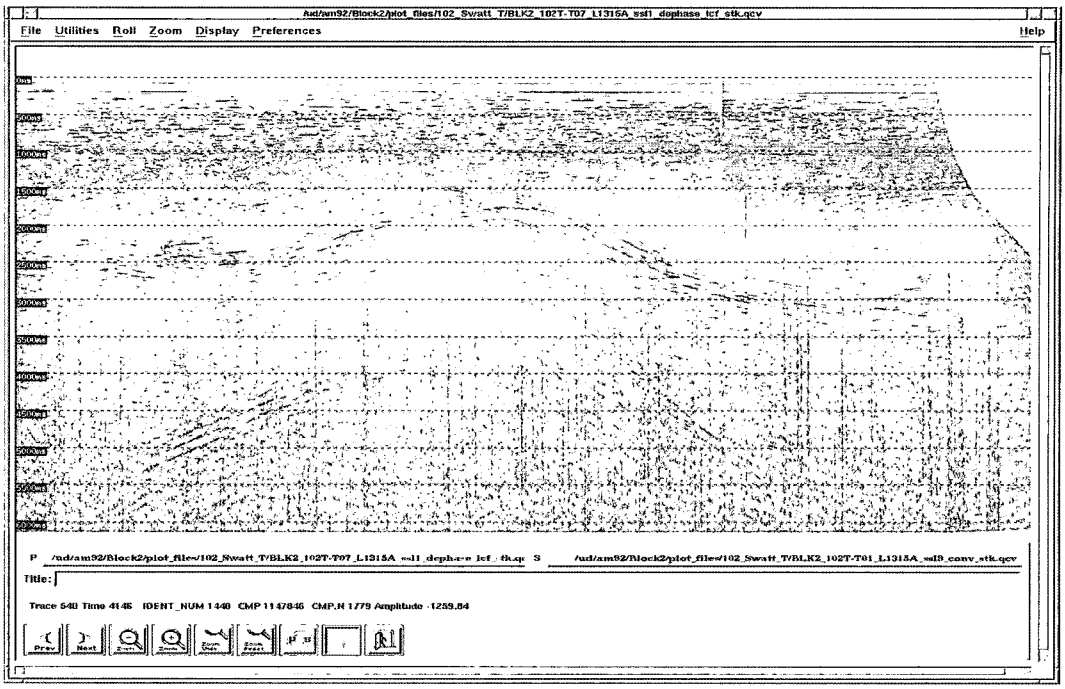

Fig. 2. Stack section which designature and 4 Hz low cut filter are applied for line 1315.

compensate the amplitude losses due to spherical divergence and inelastic attenuation. The correction, which is normally referred to spherical divergence correction, depends wholly on time. It is to correct the loss of energy from the source because the spherical wave front as the energy is transmitted down through the earth. The loss of energy is a time squared function.

Inelastic attenuation was corrected to compensate for the absorption of energy by the rock matrix due to such things as friction between particles. It is also normally a linear function and so the form of correction used for block II is V*V*T.

Swell and Strum Noise Attenuation

Two types of coherent noise causing special attenuation are guided waves and side scattered energy. Fig. 3 shows a sketch of coherent noise with primary events. The dispersive waves labeled as A in Fig. 3 are guided waves, and linear events B and C and the events D with curvature are associated with the side scatters.

These two noises, in general, can be effectively attenuated by stacking process and F/K filtering. However, as the swell attenuation process was run in the shot domain only, it was not able to remove the noises completely because they appeared across several adjacent traces (the swell attenuation program has trouble separating the noises from primary signal). After sorting into the receiver domain, the noises are distributed across several receiver gathers, and we can remove them in the second pass.

Among the noises contaminating the seismic data, the

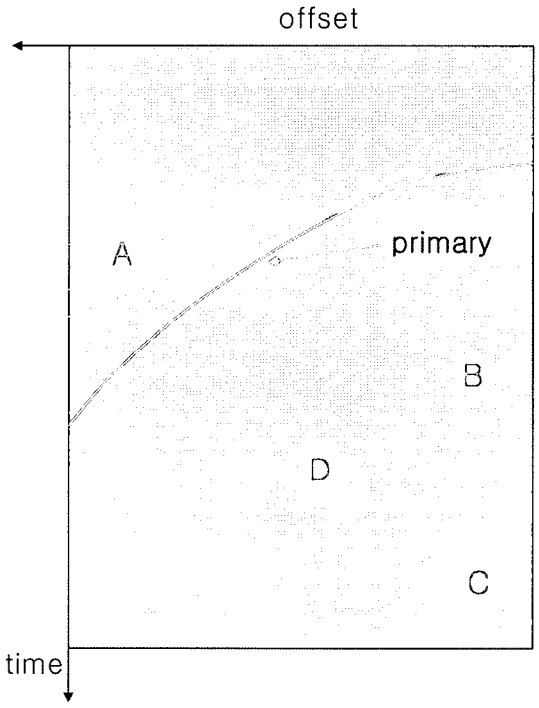

Fig. 3. A sketch of coherent noises with primaries.

strum noise is caused by oil filled section of a streamer during a typical seismic survey. It means that the solid filled sections could be free of the strum noise. On our test processes, F/K filtering process is being used to remove the strum noise shown through on the stack section. Fig. 4 shows a typical shot record with side scatters energy and strum noise caused

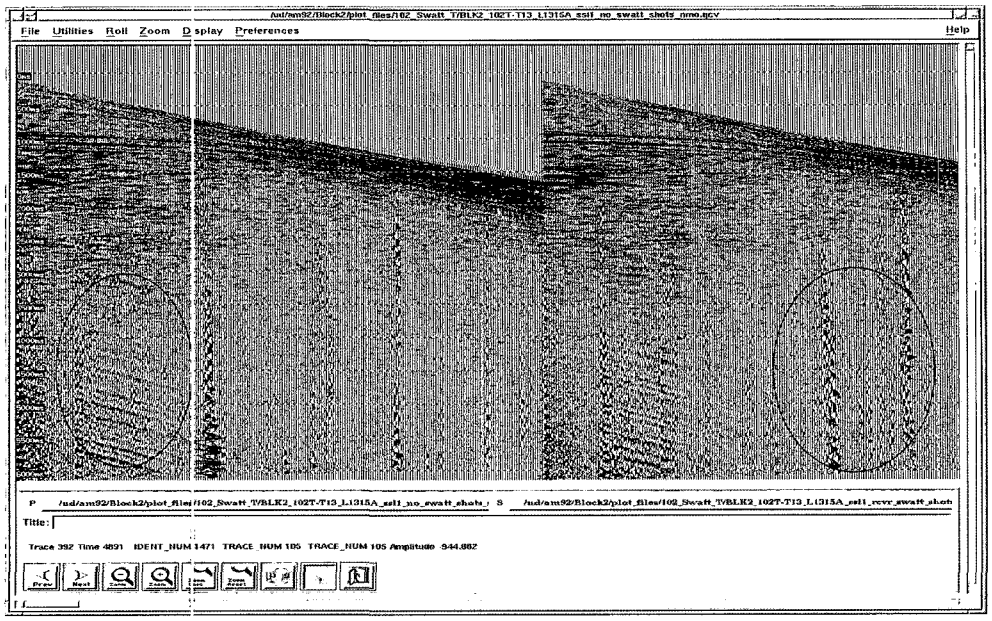

Fig. 4. Shot records which no swell noise attenuation process is applied.

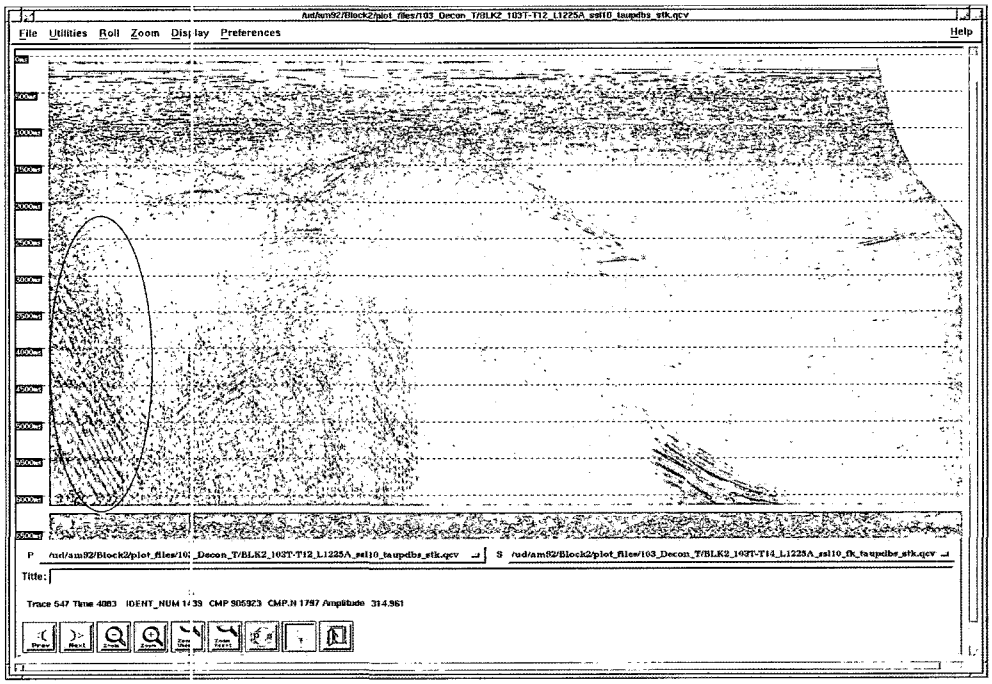

Fig. 5. Brute stack section for line 1225: Strum noise can be seen on the left below.

during survey on Block II area. The strum noise is strong enough to appear in the brute stack section (on the left below of Fig. 5).

Figs. 6 and 7 show the shot record and the stack section with F/K filtering applied. In Fig. 7, it turned out that the result after applying F/K filtering process appeared to be better than the one before. In Fig. 7, however, the strum noise could not be removed as completely as expected. Therefore, the followings will also be applied for further noise reduction as well as multiple.

Prestack Deconvolution

Deconvolution compresses the basic wavelet in the recorded seismogram, and attenuates the reverberations and short period multiples, resulting in increasing of temporal resolution and in a representation of subsurface reflectivity. The process is normally applied before stack.

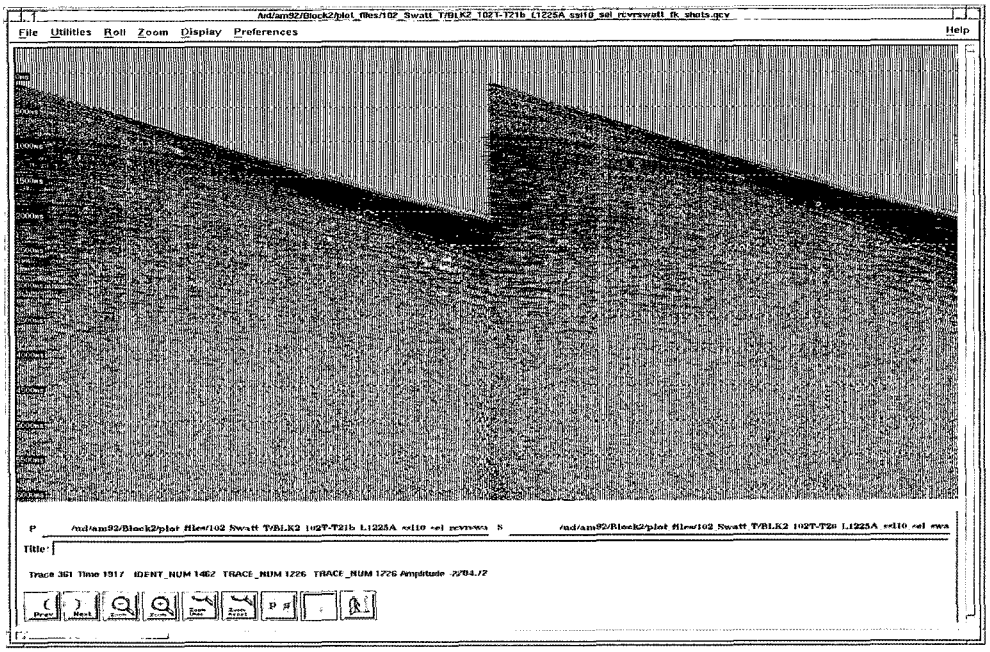

Fig. 6. Shot records which Frequency-wavenumber filter is applied.

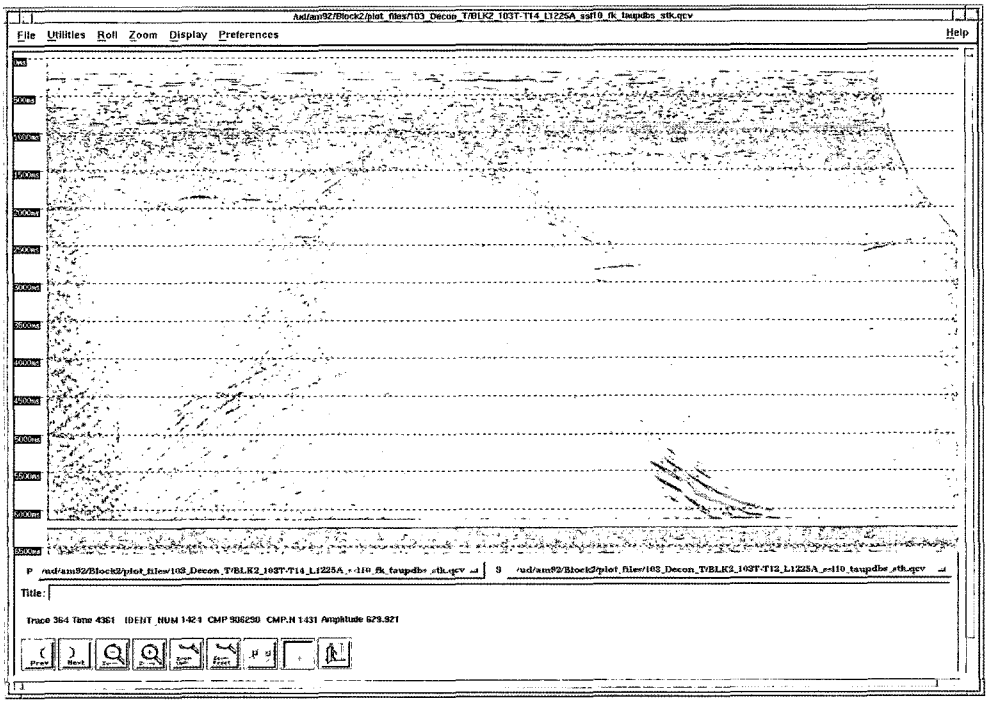

Fig. 7. Stack section which Frequency-wavenumber filter is applied for line 1225.

A comprehensive set of tests was performed using predictive deconvolution varying the gap length, autocorrelation window length, filter length and percentage white noise in the unstacked field. After testing several different gaps and operator length, 48 ms gap length with 300 ms operator length has been chosen for the better resolution. Figs. 8 and 9 show stack sections before and after deconvolution. As compared Figs. 8 and 9, the finely detailed appearance of the deconvolved section can be seen as opposed to the blurred, ringy appearance of the section without deconvolution. Especially, prominent reflections stood out much distinctly on the region A of deconvolved section. On the regions B and C, deconvolution has removed large portion of multiples but not completely. Also, for the region B, the result obtained by deconvolution

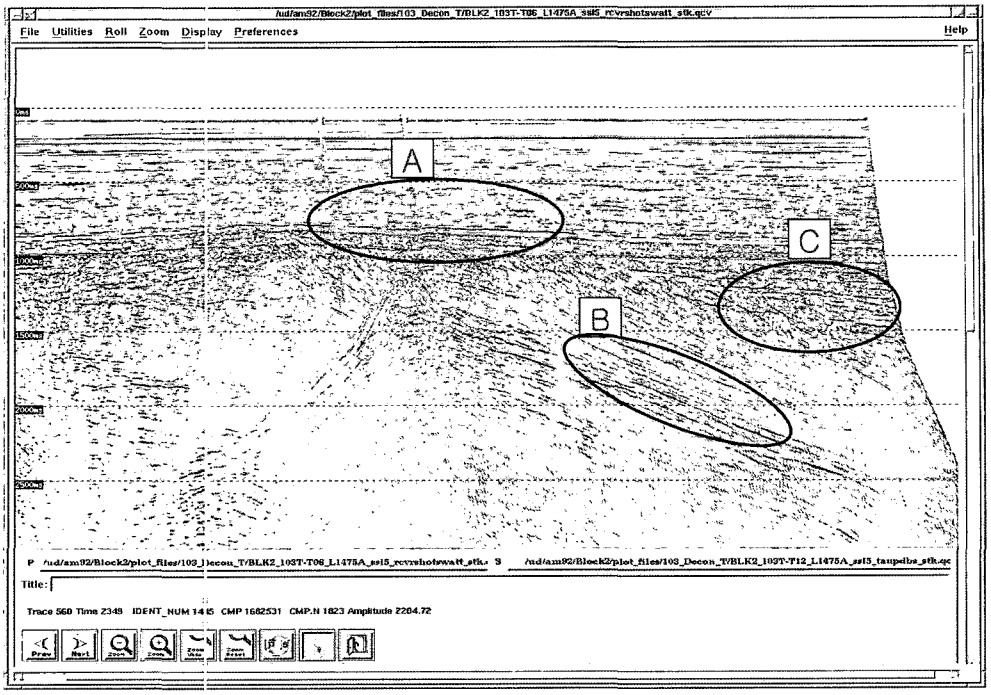

Fig. 8. Stack section which no deconvolution is applied for line 1475.

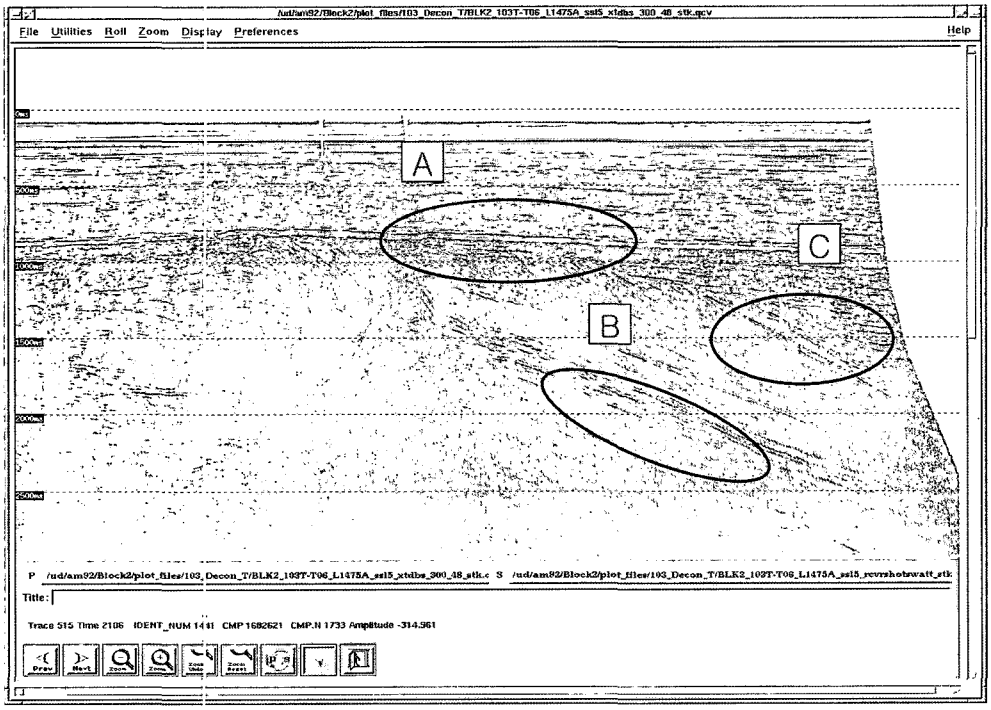

Fig. 9. Stack section which deconvolution with 48 ms gapped and 300 ms operator length are applied for line 1475.

(though it is not certain whether it is primary or not.) is not rather satisfied for the geological interpretation.

Deconvolution in τ-p Domain

After running several deconvolution processes before stack, we also applied another deconvolution in τ-p domain to attenuate the rest of multiples. The main reason for the application of this process is that conventional gaped deconvolution with several gaps and operator lengths brought out unsatisfactory results for the multiple suppression. Figs. 10 and 11 show the PSTM (post stack time migration) sections

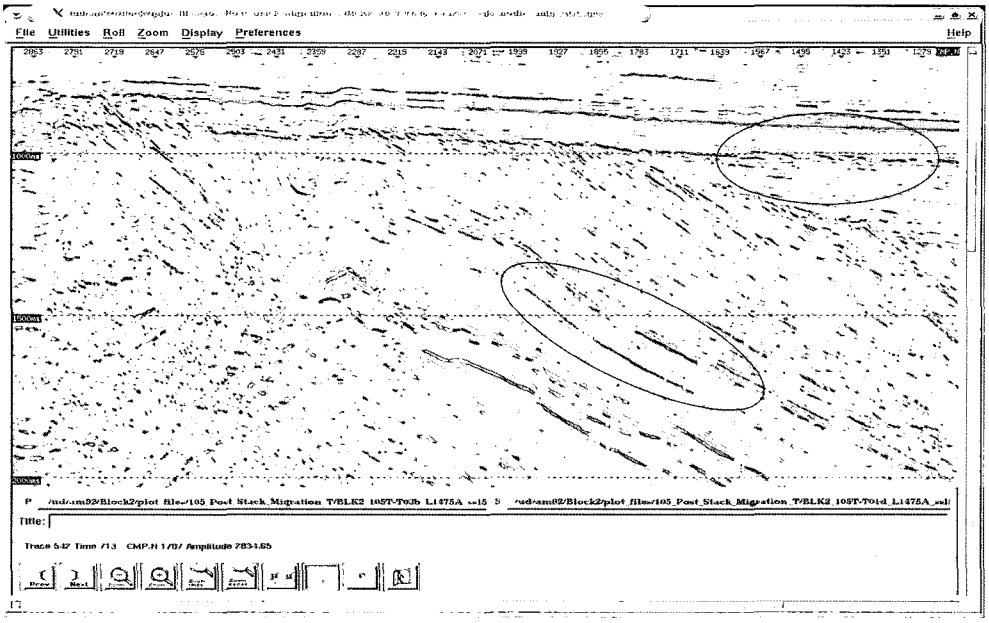

Fig. 10. Migrated section which no deconvolution is applied for line 1475.

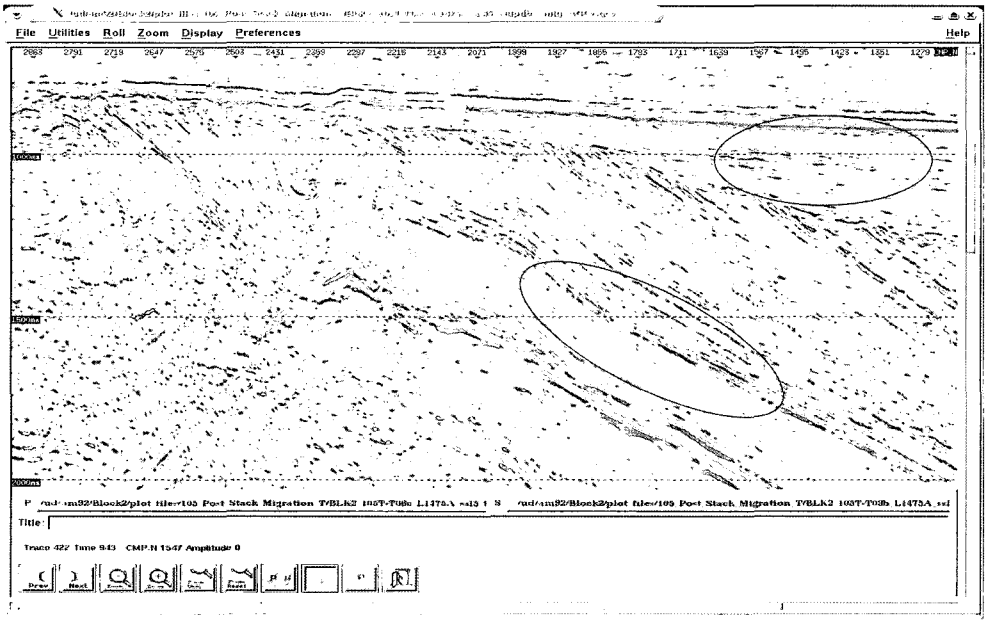

Fig. 11. Migrated section which the deconvolution in the τ-p domain is applied for line 1475.

before and after deconvolution in τ-p domain. As compared the original section before deconvolution with the best of predictive deconvolution in the τ-p domain, we can see the result that deconvolution in the τ-p domain is considerably better, and it can be successfully applied to remove the water bottom reverberations and peg-leg multiples.

Velocity Analysis

In order to determine the velocity for migration and to restore the potential primaries (these have more potential to be primaries than multiples) swept away due to the deconvolution, we analyzed the velocity more than triple at every 1 km interval. Time-velocty pick process were made by looking for the velocity that corrects any particular reflection flat within the CMP gather and then correlates this to the best stacking response.

Fig. 12 is an example of a velocity panel from the test line. The first display on the panel is the coherency plot with a velocity functions, and the second plot is the CMP gather with normal moveout correction. The last display shows the migrated image using the velocity function in the first

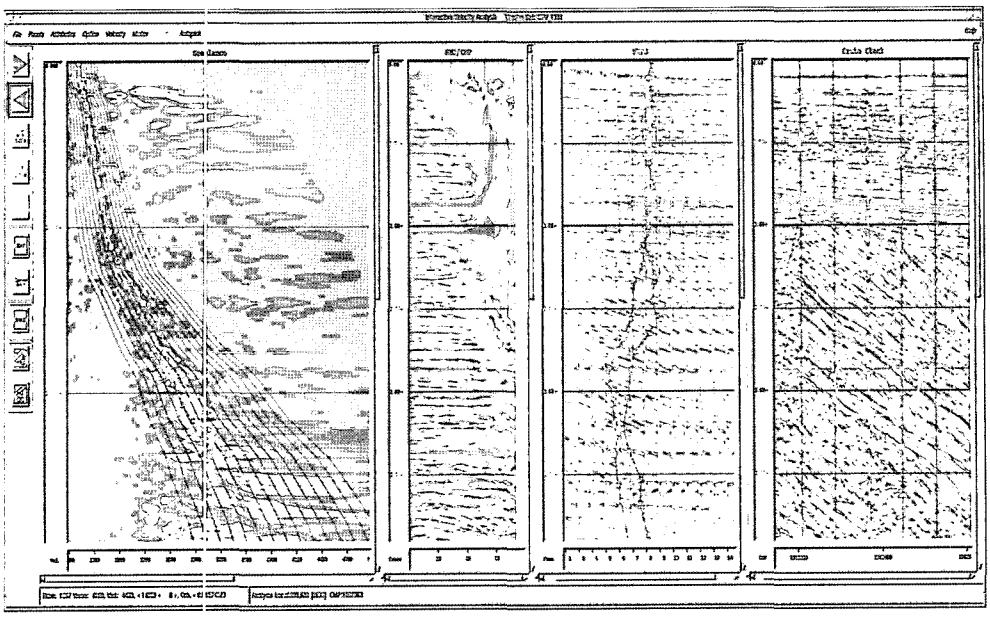

Fig. 12. Velocity analysis panel on the CMP gather space.

display. On the previous step 8, several tests have been made to attenuate the multiples and led to unexpected sweeping of such potential primaries on the circled region in this step. The circled zone, however, has a prominent improvement with such potential primary events after several trials of velocity analysis. It seems almost certain that the disappearance of the potential primary events on the step 8 is mainly due to wrong velocity picking.

Radon Demultiple

To remove the residual multiples, parabolic Radon demultiple process was conducted. On the CMP domain with NMO correction, Radon trials were initially conducted on one test line using three Radon cuts of 300, 240 and 180. The Radon cut of 300 gave better result than the others. However, after more trials for other test lines having structural complexity, it was noted that Radon cut of 240 and 180 may damage the primary events. We, therefore, chose the Radon cut of 300 as a optimum parameter for Radon process. Figs. 13 and 14 show the stack section before and after Radon process with Radon cut of 300. It was seen that Residual multiple in the circled zone was removed.

Migration

The migration test was performed using Kirchhoff algorithm. The migration velocity used were provided after third trial of MVA (not final). This process was conducted to perform the final stacking process also to analyze the migration velocity. Fig. 15 shows the prestack time migration result. Multiples have been successfully attenuated and the fault boundary is

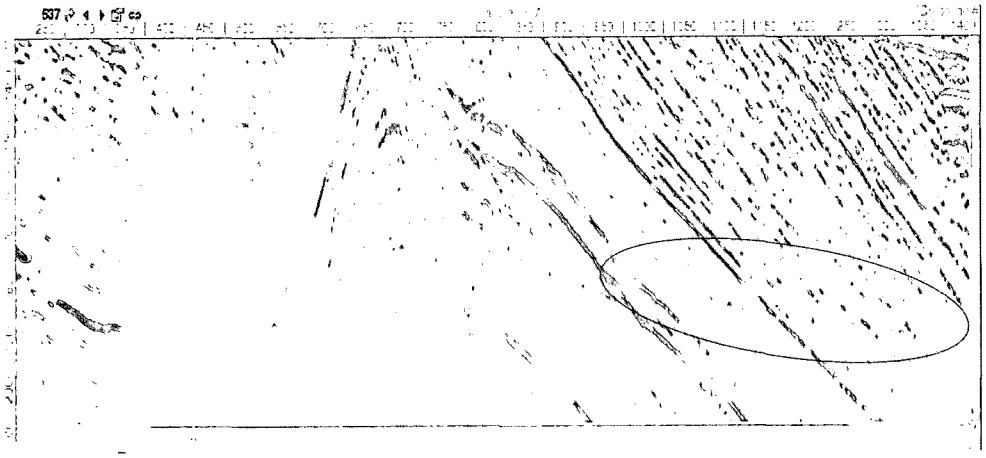

Fig. 13. Stack section which no Radon demultiple process is applied for line 1475.

Fig. 14. Stack section which Radon demultiple process is applied for line 1475.

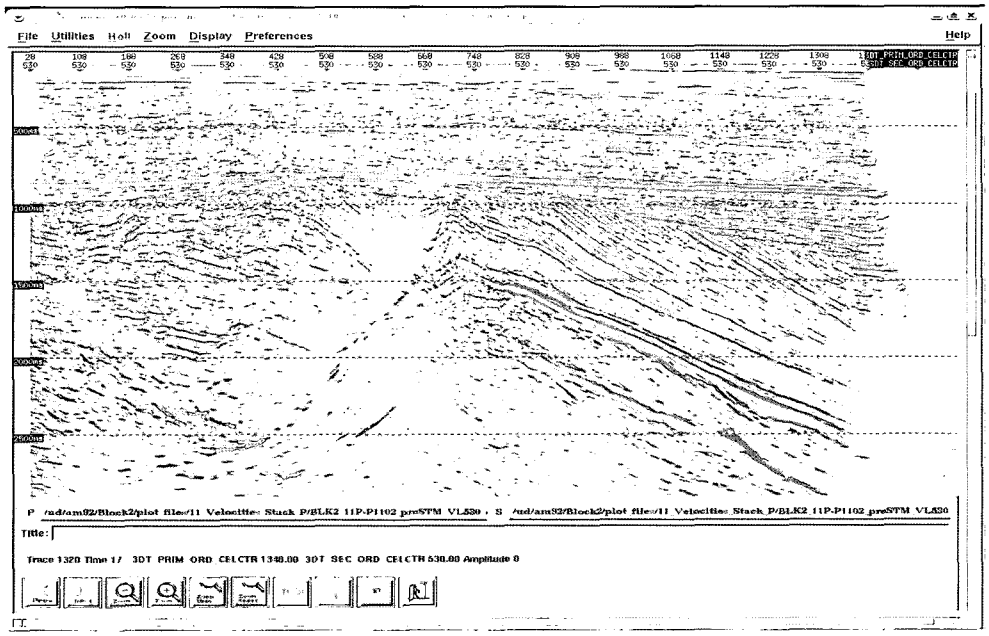

Fig. 15. Migrated image after third trial of MVA for line 1475.

defined very well.

Conclusions

After applying the processing steps, the following conclusions are obtained:

(1) For the region having the structural complexity including fault, thin layer and unconformity, demultiple processes as many as possible should be applied.

(2) Deconvolution in the τ-p domain is much better than conventional gapped deconvolution to attenuate the water bottom reverberations and peg-leg multiples.

(3) The application of deconvolution in the τ-p domain after F/K filtering has successfully removed the strum noise as well as multiples. In addition, F/K filter process should be considered mild enough not to affect the gathers requiring AVO process which will be considered in the future.

(4) It is almost certain that deconvolution process could sweep away the primary events as well as multiples. However, working on more precise process for velocity analysis, more chance of restoring the primary events could be expected.

References

Ozdogan Yilmaz, 1987, Seismic data processing.

(2005. 6. 10 원고 접수)
(2005. 7. 27 수정본 채택)